Eur. Phys. J. Appl. Phys. **56**, 34103 (2011)
DOI: 10.1051/epjap/2011110220

THE EUROPEAN PHYSICAL JOURNAL APPLIED PHYSICS

Regular Article

Molecular semiconductor-doped insulator (MSDI) heterojunctions as new transducers for chemical sensors

M. Bouvet[1,a], V. Parra[2], and J.-M. Suisse[1]

[1] ICMUB, Université de Bourgogne, CNRS UMR 5260, 9 Avenue Alain Savary, BP 47870, 21047 Dijon, France
[2] DC Wafers Investments, S.L. 24227 León, Spain

Received: 10 May 2011 / Accepted: 12 September 2011
Published online: 23 November 2011 –

Abstract. This article describes a new principle of transduction involving an heterojunction between a Molecular Semiconductor and a Doped Insulator (MSDI). Herein, we report on an MSDI-based sensor featuring an heterojunction between a lutetium bisphthalocyanine ($LuPc_2$), which acts as Molecular Semiconductor (MS) and a thin film of Doped Insulator (DI) made of substituted or fluorinated copper phthalocyanine (CuF_nPc, where $n = 0, 8, 16$). Previously, we reported the peculiar effect of the heterojunction on the MSDI's electronic behavior, suggesting this device as a new kind of transducer for gas chemosensing. Indeed, of particular significance was the key role of modulator played by the nature of the doped insulator sub-layer. While the MS thin film remains the only layer of the sensor exposed to gas atmosphere, the DI's ability to tune the electronic characteristics of the organic heterojunction allows it to drastically affect the nature of the effective charge carriers. In particular, an increase in fluorination of the doped insulator can cause an inversion of the $LuPc_2$ response toward electron accepting (ozone, ppb level) or donating (ammonia, ppm level) gases. The present work focuses on the structural, electronic and electrical properties of the MSDI heterojunction, which have been studied by UV-vis spectroscopy, atomic force microscopy, current-voltage measurements and chemical doping, in order to shed some light on this phenomenon. The unique ambipolar nature of $LuPc_2$ is suggested to be the main property responsible for the MSDI's unique behavior.

1 Introduction

Interest in molecular materials has been driven in large part by their various and prosperous applications, especially in the domain of organic electronics, where they offer many advantages as well as alternative approaches [1–4]. This is mainly due to their useful properties, such as a good solubility into common solvents, which allows low-cost and easy processing for applications in devices fabrication. Molecular materials are also incredibly rich and versatile, accounting for the large number of well-known families of low molecular weight organic molecules that can easily form interesting molecular materials [5]. Phthalocyanines, porphyrins, oligothiophenes, arenes, fullerenes ... all of them share unique electroactive properties, which can be tuned almost limitlessly by varying the molecular design, the physico-chemical nature and/or the number of their substituents and when relevant, the nature of the core transition metal, etc.

Among them, phthalocyanine derivatives, either metalated (MPc) or non-metalated (H_2Pc), are without any doubt highly interesting candidates for the development of thin film sensors and transducers [6–8]. In addition to their optical properties – they were first used as pigments – phthalocyanines are endowed with very rich electrical properties. Besides, depending on their chemical nature (central metal, peripheral substituents, etc.) phthalocyanines can behave either as semiconductor or as doped insulator (extrinsic semiconductors of *n*- or *p*-type) [9].

A special case is that of bisphthalocyanines (sandwich complexes of rare earth elements), which are stable radical molecules. Specifically, the lutetium derivative ($LuPc_2$) – the first reported intrinsic molecular semiconductor [10,11] – exhibits an uncommonly high density of free charge carriers (ca. 5×10^{16} cm^{-3}), with an unusually small energy gap (ca. 0.5 eV) giving rise to quite a high electronic conductivity at room temperature (ca. 5×10^{-5} Ω^{-1} cm^{-1}) [1,10–14].

Indeed, the conductivity σ of a *p*-type semiconductor can be approximated by $\sigma = n_p e \mu_p$, where n_p is the density of the majority charge carriers (holes) and μ_p is the mobility of carriers. Both terms are respectively related to the thermodynamics of the material and to structural parameters. The performance of a conductimetric transducer will therefore depend on the variations of those parameters

[a] e-mail: marcel.bouvet@u-bourgogne.fr

and on the work function modulation [15,16]. Usually, the gas-phthalocyanine interaction mechanism is explained by the occurrence of two successive events: the gas adsorption onto the surface of the film followed by a diffusion process into the bulk [2]. Meanwhile, surface polarization occurs causing the formation of charge-transfer complexes, which then dissociate, thus injecting charge carriers into the material. As a result, the gas-phthalocyanine interaction mechanism essentially leads to a modification of the number of charge carriers within the sensing material, which then reverberates on the measured conductivity.

Although this is well understood when considering a strong acceptor gas such as ozone or nitrogen dioxide [17,18], the effect of good electron donors such as ammonia cannot easily be supported in terms of charge carrier injection. Furthermore, given the countercharge effect that donor species have on *p*-type materials, the observed conductivity change is likely to be the result of variations in the hole trap energy (variation in charge carrier mobility) or in the charge carrier transport properties, owing to a change in the density of the electronic states [19–21]. Either way, both processes result in a change in the measured conductivity, which is taken as the primary source of sensing information.

In chemical sensors, $LuPc_2$, owing to its radical nature, can be easily oxidized and reduced. Thus, it has been used as sensing material for the detection of various gases having a wide spectrum of electron donating-accepting properties (oxidizing, reducing and even non-redox active molecules such as the volatile organic compounds, VOCs) [22,23]. Elsewhere, we have used MPcs as sensitive element for the development of chemiresistor-based sensors [24], organic field-effect transistors [25–27] and, in recent times, even *p*-*n* diodes [28,29]. In addition, high-quality performances as electrochemical liquid sensors for electronic tongues based on MPcs have also been reported [30,31]. In gas sensors, whereas *p*-type MPcs are well sensitive to acceptor gases [2,17,32,33], the detection of donor gases is devoted to *n*-type MPcs [34]. These materials are rather insulators, with energy gaps around 2.0 eV, densities of charge carriers of roughly 10^5 cm^{-3} and thin film conductivities at room temperature lower than 10^{-10} $(\Omega\ \mathrm{cm})^{-1}$, but the doping effect of redox active gases can trigger the creation of a substantial number of extrinsic charge carriers.

From this background, we recently proposed a new principle of transduction based on molecular material heterojunctions, called MSDI for Molecular Semiconductor-Doped Insulator [35]. This new transducer has been patented [36]. It is a simple device formed by a thin film-based heterostructure from unsubstituted or fluorinated copper phthalocyanine Cu(F_nPc) ($n = 0, 8, 16$), which is in contact with two interdigitated electrodes. The top layer of the device, which is the only material exposed to the outer atmosphere, is entirely constituted of $LuPc_2$ (Fig. 1). Henceforth, the corresponding MSDIs will be referred to as F0, F8 and F16, in relation to the characteristic number of fluorine atoms in the phthalocyanine-based material used as sub-layer. Both $n = 0$ and $n = 16$

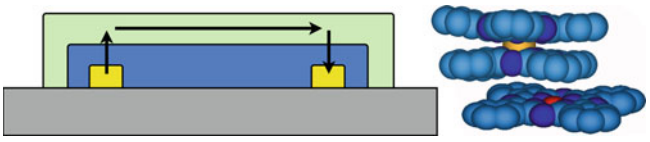

Fig. 1. (Color online) (a) Schematic side view of an MSDI heterojunction; the arrows indicate the main charges flow from one electrode to the other. (b) Compact mode view of mono- and bis-phthalocyanines.

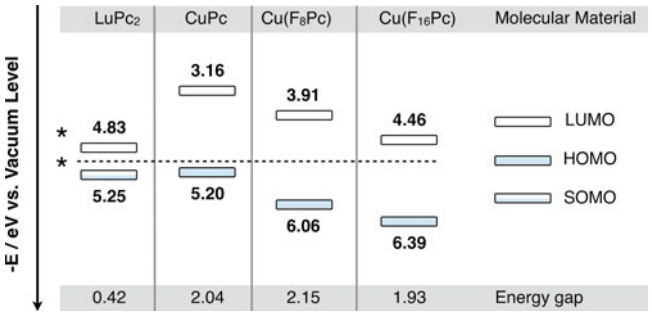

Fig. 2. (Color online) Scheme of the relative electron acceptor and donor energy levels (eV) for all phthalocyanines derivatives used as molecular materials to form the MSDI displayed in this article. The values displayed on this figure have been estimated by means of cyclic voltammetry ($\star$) in solution [12] and photoelectron spectroscopies [42].

derivatives of Cu(F_nPc) are functional materials commonly used in the field of organic electronics, owing to their efficient hole [37] and electron [38–40] transport endowment. However, much less is known about the $n = 8$ derivative [41]. We recently reported the synthesis of this non-commercially available compound [35]. From both Ultraviolet Photoemission Spectroscopy (UPS) and Inversion Electronic Photoemission Spectroscopy (IEPS) studies [42], it has been established that all three Cu(F_nPc) species possess quite comparable energy gaps. Still, and as a consequence of the rising electron withdrawing effect, the absolute HOMO-LUMO values are systematically bent downwards pursuant to the degree of fluorination of the phthalocyanine macrocycle (i.e., the electronic affinity, EA, increases).

On account of its own electronic properties, $LuPc_2$ behaves differently in the MSDI heterojunctions depending on the nature of the doped insulator used as sub-layer. The HOMO and LUMO levels of the Cu(F_nPc) species are compiled in Figure 2 and compared to those of $LuPc_2$ [12,42,43]. Besides the enhanced conductivity of the heterostructures (compared to that of the respective single-layer films), the gas sensitivity of $LuPc_2$ can be strongly modulated, even inverted, depending on the degree of fluorination (the electron affinity) of the underlying Cu(F_nPc) sub-layer. Albeit a $LuPc_2$ resistor exhibits a linear behavior of its *I*-*V* characteristics, the MSDIs show nonlinear but symmetrical *I*-*V* curves. The energy barrier is higher for F16 due to the nature of the majority charge carriers, namely negative in F16 and positive in $LuPc_2$. Fittingly, F8 leads to an intermediate electrical signature.

https://doi.org/10.1051/epjap/2011110220 Published online by Cambridge University Press

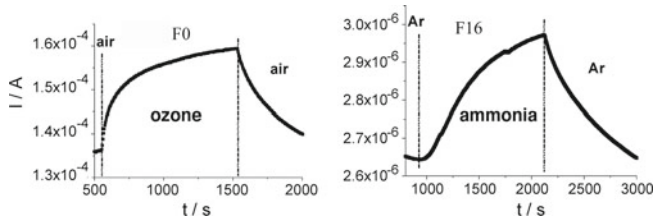

Fig. 3. Typical sensing current response of F0 and F16 MSDIs when exposed, respectively, to 90 ppb of O_3 (alternately with pure air) and 35 ppm of NH_3 (alternating with argon).

We also demonstrated previously that the association of other doped insulators to $LuPc_2$, in an MSDI heterojunction, provides well-defined gas sensors. Thus 5,5′-dihexyl-α,ω-sexi-thiophene and N,N'-dineopentyl-3,4,9,10-perylenetetracarboxylic-diimide used as sub-layers instead of CuPc or $Cu(F_{16}Pc)$, led to well-characterized MSDIs of p-type and n-type, respectively [44].

The measured current of the p-MSDIs that were prepared with a p-type doped insulator as a sub-layer increases under O_3 (90 ppb), and decreases under NH_3 (35 ppm). The reverse effect is observed in case of F16. The positive responses of F0 to O_3 and of F16 to NH_3 are shown in Figure 3. This electrical behavior is related to the density of majority charge carriers, which increases under O_3 and decreases under NH_3. On the contrary, n-MSDIs, prepared with an n-type doped insulator as a sub-layer, experience negative responses to O_3 and positive responses to NH_3, as a result of an increased energy barrier across the MSDI interface. Thanks to the singular redox properties of $LuPc_2$ used as the top layer in all the studied MSDIs, all heterostructures display high sensitivity while improvingly lacking the saturation effect observed in $LuPc_2$ resistors [1,17].

The present work entails both fundamental and applied research aspects. So far, MSDI heterojunctions have only been scarcely studied [45] never accounting for the effect of gases despite the fact that sensor characteristics have been known to be impacted by the thin-film structure of the molecular materials [15,46,47].

Henceforth, and along with the fundamental characterization of the electrical properties obtained from the current-voltage experiments we reported previously [35], this article will discuss the structural and chemical properties of the new MSDI devices in relation to their peculiar behavior. Specifically, all hererojunctions will be studied after exposition to high concentration of NO_x vapors. Their behavior following exposure to redox active gases such as ozone (O_3), the leading oxidizing agent in the urban pollution [48] and to electron donor gas like ammonia (NH_3) (to be monitored for indoor pollution control and industrial emission issues management [49,50]), provides valuable information for the future development of new sensors and/or detectors. Along this line and owing to the MSDI's enhanced sensing performances, such experiments unveil new perspectives on the improvements of selectivity profiles, which is one among the main drawbacks of all sensor devices. The dependency of the electronic properties of $LuPc_2$ semiconductor on the effect exerted by the doped insulator layer at the heterojunction level is also studied.

2 Experimental

2.1 Molecular materials

CuPc was purchased from Fluka. $Cu(F_{16}Pc)$ [51,52] and $LuPc_2$ [53–55] were synthesized according to previously reported methods. Conversely, we synthesized the 2,3,9,10,16,17,23,24-octafluorinated phthalocyanine $Cu(F_8Pc)$ by reaction of 4,5-difluoro-1,2-dibromobenzene with copper cyanide in dimethylformamide [35].

2.2 Devices

All heterojunctions were built by successive deposition of the corresponding molecular materials onto Au/Si (polycrystalline, 1.0 × 1.0 cm) and ITO/glass (1.1 × 0.9 cm substrate, sheet resistance 10 Ω cm^{-1}) interdigitated electrodes (separated by 10 and 75 μm, respectively), by means of classical thermal evaporation (using a VEECO 770 system) from two tantalum boats, at the rate of ca. 10^{-6} mbar, and 2 Å s^{-1}. Care was taken not to break the vacuum between each step. The thickness of 100 nm for each layer was controlled by two quartz crystal microbalances located independently in the vicinity of their respective boat. The organic device, in which the $LuPc_2$ material is the only surface exposed the gases, is depicted in Figure 1. Additionally, a $LuPc_2$ single-layer resistor (100 nm, on ITO/glass) has been prepared to serve as a reference and has been handled in near identical conditions, for comparison purposes.

2.3 Samples treatments

In order to oxidize the samples, all newly prepared MSDIs underwent extreme NO_x vapors treatment (direct exposition to fuming from a nitric acid solution) for 30 min prior to UV-vis observation and electrical properties characterization.

2.4 UV-vis characterization

The UV-vis spectra of the ITO-deposited samples were registered using a Shimadzu UV-2101 spectrometer, between 900 and 400 nm. A bare ITO/glass substrate was used as a reference.

2.5 Atomic Force Microscopy (AFM)

Tapping Mode AFM (TM-AFM) images of the ITO-based samples were recorded by the commercially available AFM equipment, Multimode Nanoscope III, at room conditions.

https://doi.org/10.1051/epjap/2011110220 Published online by Cambridge University Press

2.6 Electrical measurements

All fundamental electrical and sensor measurements were performed at room temperature using a 6517A Keithley electrometer equipped with an embedded DC voltage supply. The electrometer was controlled through a custom-made software relying on a GP-IB bus connection for data communication. Current-voltage (*I-V*) curves were registered with voltage values ranging from −10 V to +10 V while taking care to start and finish at 0 V bias (in order to avoid any irreversible polarization effect) except for gas sensing experiments, during which the samples were constantly polarized at +1 V. All experiments were performed in dark conditions to avoid any photoelectric effects that may have occurred otherwise.

2.7 Gas sources for sensing experiments

Ozone was generated using an analyzer/generator (O_3 41M Environment SA) capable of supplying a controlled flow of ozone in air at the ppb level (total mass flow: 1.6 L min^{-1}). A flow of clean air was used as purging gas. In case of ammonia, gas from a standard bottle (1000 ppm in Ar, from Air Liquide, France) was diluted with dry Ar using mass flow controllers (total mass flow: 0.5 L min^{-1}) in order to reach stable, controlled and adjustable ammonia concentrations.

3 Results and discussion

3.1 AFM measurements

AFM provides information on the aspect of the films and will allow us to correlate the optical properties from the studies mentioned below with morphological data. In particular, and given the observed UV-vis features of the MSDI heterostructures exposed in 3.3.2, their involvement in arrangement in films is interesting. Figure 4 illustrates a series of tapping mode AFM images of the F0, F8 and F16 heterostructures deposited on ITO/glass electrode substrates. Line profile analyses are included, in order to assist with the morphological study.

The AFM image of the heterostructure F0 (Fig. 4a) reveals a granular structure (polycrystalline aggregates) characteristic to that of phthalocyanine films. In particular, deep pores averaging 45 nm high separate regular-sized $LuPc_2$ grains. This suggests an upward growth of $LuPc_2$ from the CuPc substrate. All these features are homogeneously distributed across the scanned surface, resulting in a roughness of $R_q = 15$ nm.

Somehow, the aspect of the sample F8 is different (Fig. 4b). In this particular case, given the fact that the polycrystalline grains are shorter and wider, a modified, two-dimensional growth mechanism can be considered. The previously observed porous pattern is now replaced by a smoother surface with a roughness $R_q = 12$ nm. It is worth mentioning at this point that given the complex nature of the device (ITO patterned glass, then $Cu(F_nPc)$, then $LuPc_2$), a roughness of 12 nm is not a very large value. Analysis of the heterostructure F16, however, reveals that the deposition of $LuPc_2$ over the perfluorinated phthalocyanine leads to a distinctive film morphology (Fig. 4c). The actual roughness increases noticeably ($R_q = 44$ nm), resulting in thicker and wider crystalline aggregates than those observed on F0 and F8 heterostructures. This distinct morphology was uniformly found on wider surface scans. Therefore, the $Cu(F_nPc)$ substrates definitely have a template effect for the growth of the subsequent 100 nm thick $LuPc_2$ film. $Cu(F_{16}Pc)$ is indeed known to form islands with an energetically favored upright-standing orientation [39,40]. This would promote the growth of large polycrystalline aggregates of $LuPc_2$ from the very first molecular layers, while progressively increasing the roughness of the film [56,57] and its specific surface.

Such topography also corroborates previous observations of CuPc films over ITO [58]. Nonetheless these trends contrast with the less uneven film of $LuPc_2$ in the F8 heterostructure, suggesting that $LuPc_2$ stands in a rather segregated fashion on top of the regular $Cu(F_8Pc)$ layer.

3.2 The effect of doping on the heterojunctions

3.2.1 UV-vis spectroscopy

UV-vis spectroscopy quickly provides valuable structural information, especially when dealing with phthalocyanine-based thin films [15]. The 400–900 nm region contains some of the most representative absorption bands for both the mono- and bisphthalocyanines, such as the so-called *Q*-band, which arises between 600 and 800 nm from the $\pi \rightarrow \pi^*$ charge-transfer transition of the Pc ring system, and the "blue vibration band" (BV) [59] near 470 nm, which involves the transition $e_1 \rightarrow a_2$ (associated with the Semi-Occupied Molecular Orbital (SOMO) of the $LuPc_2$ neutral radical). Figure 5 represents the UV-vis spectra of the F0, F8, F16 heterostructures. No significant change in both *Q* and BV bands of $LuPc_2$ occurs through the series, suggesting that both semiconductors keep their bulk electronic identity at the steady state.

The UV-vis spectrum of the heterostructure F0 exhibits an intense band centered on 672 nm that can be attributed to the typical $LuPc_2$ *Q*-band (vide infra). Usually, the *Q*-band for $LnPc_2$ molecules in their neutral "green-form" is well defined, with high relative intensities, even when processed in thin film [60,61]. However, this is not always true for films of MPc. Two additional bands around 617 nm and 730 nm (shoulder) can respectively be attributed to the monomer and dimer CuPc *Q*-band splitting absorptions.

The heterostructure F8, to a large extent, shares a similar UV-vis band profile. As for F16, an additional band shows up (close to the NIR region, at 787 nm), that could be assigned to a charge-transfer exciton state between pairs of edge-to-edge adjacent molecules within the film [15,62,63]. Such observation is typical to crystalline forms of perfluorinated phthalocyanines [64]. The $LuPc_2$

https://doi.org/10.1051/epjap/2011110220 Published online by Cambridge University Press

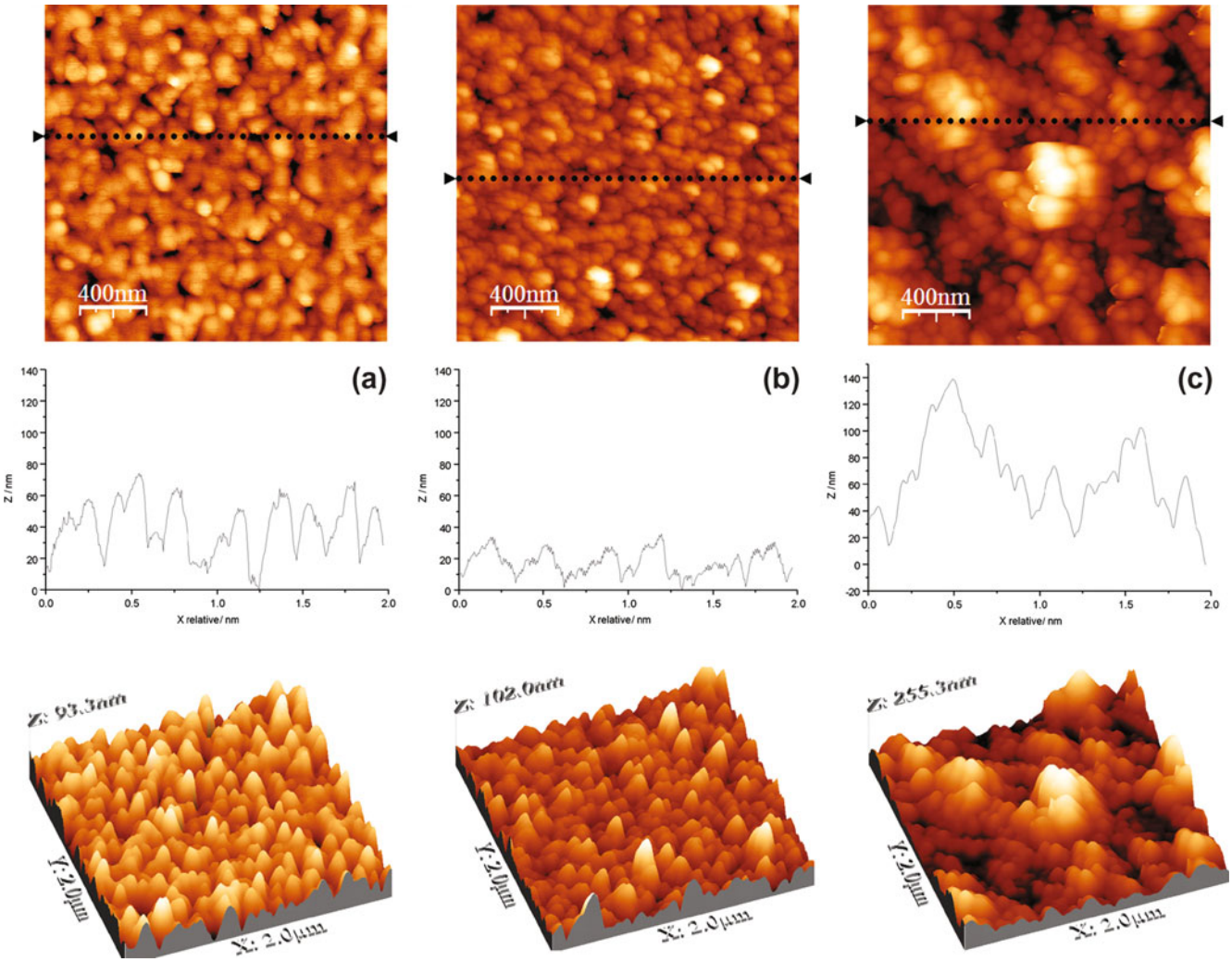

Fig. 4. (Color online) Typical TM-AFM images (2 μm $\times$2 μm) of the MSDI heterostructures. Relative height (Z) profiles as well as 3D representations are included. (a) F0; (b) F8; (c) F16.

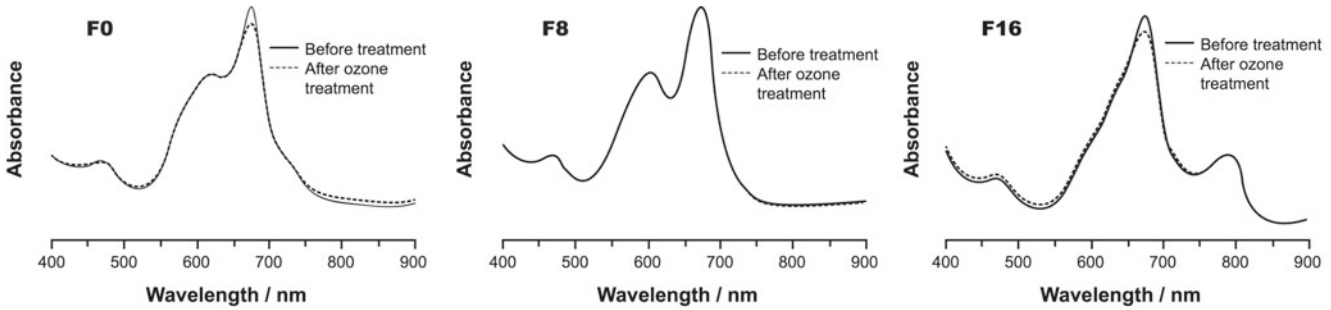

Fig. 5. UV-vis absorption patterns of the heterostructures F0, F8 and F16 deposited on ITO glass substrates, after 50 min of exposure to high concentration of O_3 in air (1000 ppb, dotted line).

Q-band is also much better resolved. This kind of behavior is most probably the result of a specific molecular arrangement of Cu(F_{16}Pc).

Globally, the $LuPc_2$-related Q and BV bands energy seems to remain practically unaltered in the MSDI, whereas their relative intensities, regarding those of the phthalocyanine sub-layers, are distinctively distributed. This is a result of the dependence on the number and the orientation of the nearest-neighbor molecules in the film structure, mainly at the organic interface level [65,66]. Thus confirming the eventuality of a template effects from the Cu(F_nPc) sub-layer on the arrangement of $LuPc_2$ during the initial stages of growth [67,68]. Ultimately, the effect of the exposure to ozone (a very strong and

https://doi.org/10.1051/epjap/2011110220 Published online by Cambridge University Press

efficient oxidizing agent) was checked prior to the gas sensing experiments. All samples were submitted to a high concentration of ozone (1000 ppb) for 50 min. Interestingly the doping induced by ozone did not give rise to any noticeable change in the UV-vis spectra of the heterostructures (Fig. 5). This result implies that all films are quite stable, even after a very strong ozone treatment, which is rather advantageous for a potential use as ozone sensor. Furthermore, this observation also indicates that the effect of ozone remains localized at the surface and that there is no diffusion into the bulk, as previously exposed by one of the authors of this paper, by means of X-ray Photoelectron Spectroscopy (XPS) [25].

Exposition of $LuPc_2$ thin films to bromine vapors or to those of nitric acid (hereafter NO_x) has been reported to cause significant alterations in its UV-vis absorption spectrum, leading to the so-called oxidized "red-form" of the bisphthalocyanine [22,69]. Herein a similar experiment was performed on the MSDI with the sole purpose of studying the $LuPc_2/Cu(F_nPc)$ heterostructures using a different approach, in the hope of obtaining complementary data on the heterojunction effect in MSDI devices.

Intriguingly, and despite the fact that a dark green film of radical neutral $LuPc_2$ material turns reddish after NO_x exposure, the original greenish F0, F8, and F16 films turned out to become respectively reddish-purple, dark blue-purple and dark teal. Such observations confirm that the previously reported peculiar properties of $LuPc_2$ in the MSDI heterojunction [35] are indeed predetermined by the nature of the sub-layer, even though the latter is not exposed to gas atmosphere.

The UV-vis spectra of Figure 6 clearly show the modified absorption patterns. For comparison purposes, two spectra of $LuPc_2$, before and after undergoing the same doping process, are included as well. Table 1 collects the absorption bands related to the NO_x treatment. As a preliminary conclusion, it is now possible to assign the most intense band (the one around 675 nm) to the $LuPc_2$ Q-band (inset of Fig. 6), since it is shifted to the neighborhood of 700 nm for all heterojunctions in the series.

A more careful analysis of the energy, shape and relative intensity of the UV-vis bands reveals that the behavior of $LuPc_2$ in its typical red-form (when in single layer) is mainly conserved in F0. This is most probably the result of the juxtaposition of two p-type materials in the heterostructure. The same remark does not apply to F8 and F16, where the use of fluorinated phthalocyanines leads to an increased energy barrier across the junction.

Additionally, the effect of the exposure to NO_x on the MPc underlying films is not as drastic as on $LuPc_2$, even considering the large amount of time allowed for the NO_x doping process. This is especially true for fluorinated MPcs, which seem to sustain negligible changes, accordingly to their marked acceptor character. Evidences to support this claim can be found, for instance, in the steady CT-band of F16 (centered on 787 nm) or in the MPc Q-band (600 nm) for F8. To further investigate this matter, NO_x treatment was performed on MPc single layers (see Fig. 7). After exposure, the non-fluorinated MPc was the only one to show evident signs of oxidation as seen from the important blue shift and modifications in the intensity of the Q-bands.

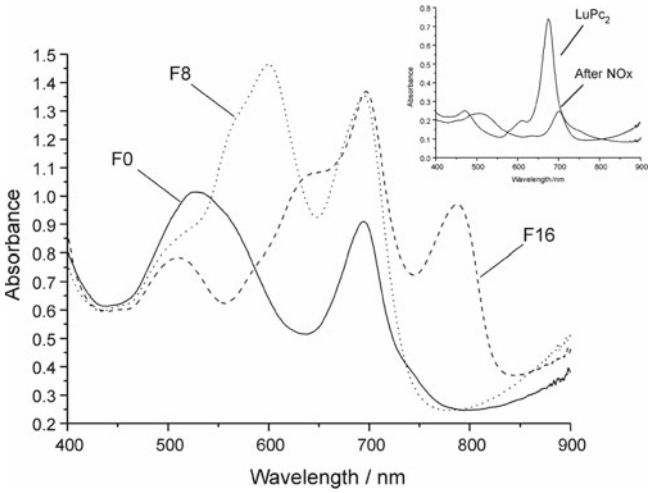

Fig. 6. UV-vis absorption spectra of the F0, F8 and F16 heterostructures deposited onto ITO, taken after the 30 min exposure to NO_x vapors. The inset on the right displays UV-vis absorption spectra of a $LuPc_2$ layer before and after undergoing the same experiment.

3.2.2 I-V characteristics

As expected, the changes induced by the oxidizing vapors of NO_x on the UV-vis absorption spectra are translated into particular I-V features. After exposure, the F16 heterojunction turns out to become more resistive by a factor of 10 (Fig. 8), owing to an increase of the energy barrier at the interface between $LuPc_2$ and the n-type sub-layer. In contrast, the conductivity of F0 is drastically increased, up to more than two orders of magnitude, as a result of the doping effect. Again, F8 exhibits an intermediate behavior, only experiencing a moderate increase of conductivity. These results are in agreement with the distinct electronic densities of $LuPc_2$ within each heterojunction.

3.3 Discussion

It is well known that following the contact between two molecular materials having dissimilar HOMO and LUMO levels, an accumulation of electron and holes at both sides of the interface occurs (space charge layer), instigating the formation of an interface dipole as well as a band bending [70–73]. In this respect, recent surface potential measurements have shown that, when forming the heterojunction, an electron displacement from the p-type material to the n-type one occurs [74].

Herein, we are dealing with $LuPc_2$, an intrinsic semiconductor, which exhibits a much higher density of free charge carriers than the MPc insulators. $LuPc_2$ is also

https://doi.org/10.1051/epjap/2011110220 Published online by Cambridge University Press

Table 1. Wavelength values and relative intensities of some of the main UV-vis bands for the heterostructures and a $LuPc_2$ single-layer film deposited on ITO/glass substrates after 30 min of NO_x vapors exposure. A non-treated $LuPc_2$ film is also included as reference.

Phthalocyanine film samples	Assignment (nm)			
	BV	MPc *Q*-band	$LuPc_2$ *Q*-band	MPc CT-band
F0	528 m	–	694 s	–
F8	510 s	600 h	694 m	–
F16	509 s	640 m	697 h	787
$LuPc_2$ (SL)	507 m	–	700 s	–
$LuPc_2$ (SL) non-treated	471	–	675 h	–

SL: single-layer; s: short relative intensity; m: medium relative intensity; h: high relative intensity.

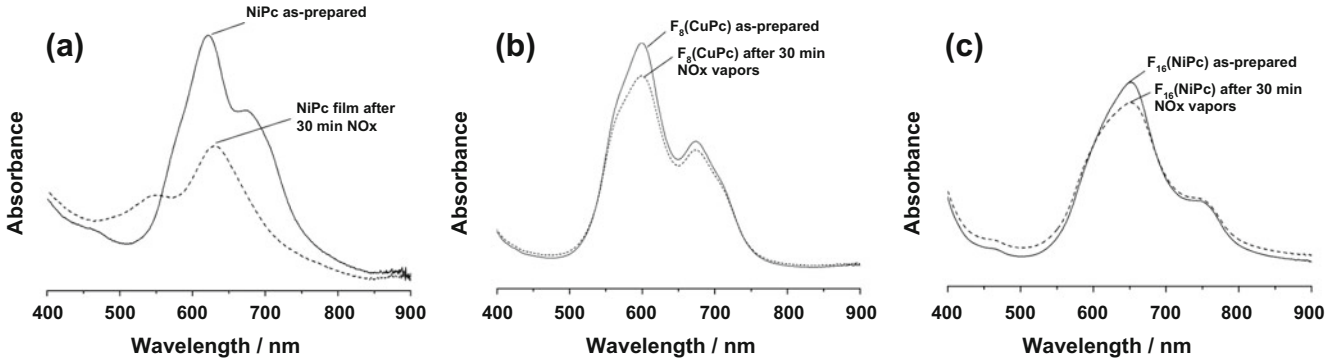

Fig. 7. Evolution of the UV-vis absorption patterns of some MPc single layers after a 30 min-long NO_x vapor exposure.

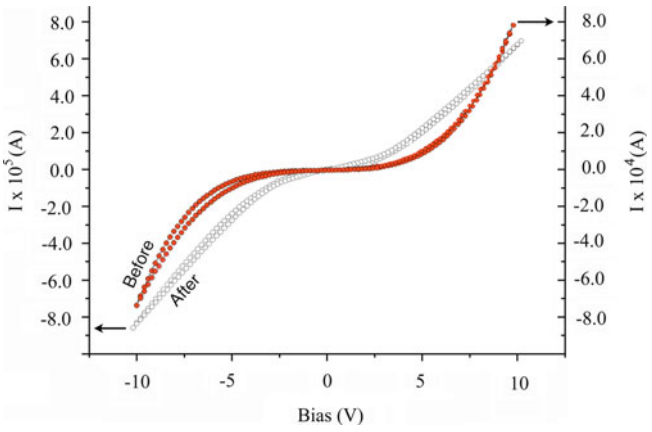

Fig. 8. (Color online) Room temperature *I-V* characteristics of the F16 MSDI device, before and after NO_x treatment.

endowed with an exceptionally small energy gap, residing almost entirely in between the HOMO-LUMO gap of the $Cu(F_nPc)$ materials, as depicted in Figure 2. This is of crucial importance and as a direct consequence $LuPc_2$ exhibits an increasingly (decreasingly) accepting (donating) behavior according to the higher (lower) EA in relation to the fluorination degree of the MPc within sub-layers.

Therefore, the MSDI heterojunctions offer new perspectives, since the bisphthalocyanine acts as a good electron donor (*p*-type semiconductor) but also, in a non-negligible fashion, as an acceptor.

This phenomenon has successfully been exploited in the realization of an ambipolar charge transport (both *p*- and *n*-channels) in FETs devices, since the accumulated countercharges can easily be driven toward the active layer of the organic heterojunction [75,76].

HOMO-LUMO energy level considerations also explain why the doping of the semiconducting layer ($LuPc_2$) is capable of changing the electrical response of the MSDIs. In the MSDI devices, only the molecular semiconductor layer is exposed to the atmosphere. Meanwhile, the buried doped insulator acts as a modulator of the nature of the effective charge carriers, by tuning the electronic characteristics of the organic heterojunction.

Clearly the MSDI heterojunction plays a key role in the device's behavior. This is the basic underlying principle of a new mode of transduction.

In $LuPc_2$ and CuPc, the majority charge carriers are positive. Thus, the current is mainly limited by the migration of charges through the less conductive material (DI). The effect of O_3 on F0 is to increase the density of the positive charges, which in turn increases the current flowing through the device. NH_3 has the exact opposite effect. The observed current decreases consequently to a drop in number of the majority charge carriers.

Owing to the high electron affinity of $Cu(F_{16}Pc)$, electron injection is easier in F16 than in F0. Subsequently, the majority charge carriers are negative in F16. Thus, the high density of opposite charges accumulated at both side of the interface leads to a higher barrier energy and to a lower current.

https://doi.org/10.1051/epjap/2011110220 Published online by Cambridge University Press

In such case, the MSDI behaves just like two consecutive *p*-*n* junctions in reverse disposition (*n*-*p*-*n*) and the current flowing from one electrode to the other is limited by the migration of minority charge carriers through $LuPc_2$. Thus, when F16 is exposed to O_3, the density of positive charges increases in $LuPc_2$, leading to an increase of the energy barrier. On the contrary, when F16 is exposed to NH_3, the energy barrier decreases and the measured current increases. It is even likely that the majority charge carriers in $LuPc_2$ actually turn from positive to negative because of its ambipolar behavior, being a radical molecular semiconductor.

All the aforementioned morphological and spectroscopic studies explain the behavior and sensing properties of the MSDIs. F0 exhibits a drastic increase of conductivity under ozone, as a consequence of the oxidation of $LuPc_2$. The sensing performance of F0 is highly improved thanks to the free holes reservoir at the $LuPc_2$/CuPc interface.

On the contrary, F16 exposition to O_3 gives rise to a significant decrease in current, even though the only layer exposed is $LuPc_2$. Analogously, ammonia is known to induce a decrease in the conductivity of *p*-type phthalocyanines [2,24,33,77] while *n*-type phthalocyanines exhibit a higher conductivity when interacting with this electron donor gas [28,34].

Still, fluorinated phthalocyanines are found to become quite resistive when operating in real-world conditions, since their negative charge carriers are vulnerable to charge trapping by ambiant atmosphere-contained species [28,78,79].

Then again, owing to its natural *p*-type semiconducting behavior, $LuPc_2$ exhibits a decreased conductivity after exposition to donor gases. As shown before under ozone, such a well-defined trend is modulated by the effect induced by the Cu(F_nPc) sub-layers.

When exposed to 35 ppm of ammonia in Ar atmosphere, a value that is lower than the usual detection threshold of indoor air quality monitors [50], each MSDI device exhibits a response of its own. Both F0 and F8 experience a drop in conductivity, a similar behavior to that of $LuPc_2$ single-layer devices. However F8 exhibits lower drop than F0. In contrast, F16 displays a totally reversed response. The current rises and the sensitivity is drastically increased.

4 Conclusion

In this work, we investigated the structural characterization, UV-vis spectroscopy, chemical doping effects and the sensing behavior toward both acceptor (O_3) and donor (NH_3) gases of the MSDI heterojunction, with emphasis on understanding the recently exposed interface effects [35] in relation to the unique electronic properties of $LuPc_2$ and its role in the peculiar response of the MSDI toward both electron accepting and donating species.

Both *I*-*V* and UV-vis studies bring new perspectives toward an exciting scenario regarding the sensing properties of the heterojunctions and their potential application as a new kind of gas transducers. Furthermore, from this work, it appears that investigating the electrical response of the heterojunctions subsequently to controlled exposition to electron accepting and donating atmospheres opens the door to a new line of research. It seems to be an excellent way toward accessing the fundamental properties of these devices, and broadly, could provide new means of studying heterostructures and junctions in the field of organic electronics fundamental research. In addition, and in the field of applied research, MSDI heterostructures had never been considered as gas sensor. Although the MSDI samples investigated in this article require an additional optimization stage for real-world applications, they do raise new perspectives in the field of organic-based gas sensors and detectors while offering the hope for improved performances (compared to that of the well-known single-layer chemiresistors).

Moreover, the MSDI heterojunction setup allows for tuning the electrical behavior of the compound interacting with the gas atmosphere. In particular, a variation in thickness of both layers will yield distinct morphologies. This should strongly influence both the electrical behavior and the sensing performances of the new transducer. Not only can this be accomplished with traditional molecular materials, such as phthalocyanines, but it can also be done with other electroactive materials [44] that possess different properties.

The authors would like to acknowledge the Agence Nationale de la Recherche (A.N.R. France) for funding and support within the POLL-CAP project (Grant No. Blan-06-154000). They also acknowledge both Dr. N. Battaglini and Dr. M.L. Rodríguez-Méndez for performing the AFM experiments as well as for supplying the electrode substrates. Finally, the authors thank Dr. J. Brunet and Prof. A. Pauly for the thin films evaporations.

References

1. M. Bouvet, in *The Porphyrin Handbook*, edited by K.M. Kadish, R. Guilard, K. Smith, vol. 19 (Academic Press, Boston, 2003), p. 37
2. M. Bouvet, A. Pauly, in *The Encyclopedia of Sensors*, edited by C.A. Grimes, E.C. Dickey, M.V. Pishko, vol. 6 (American Scientific Publishers, Valencia, CA, 2006), p. 227
3. M.L. Rodriguez-Mendez, in *The Encyclopedia of Sensors*, edited by C.A. Grimes, E.C. Dickey, M.V. Pishko, vol. 9 (American Scientific Publishers, Stevenson Ranch, CA, 2006), p. 111
4. J.T. Mabeck, G.G. Malliaras, Anal. Bioanal. Chem. **384**, 343 (2006)
5. J. Simon, P. Bassoul, *Design of Molecular Materials: Supramolecular Engineering* (Wiley, Chichester, New York, 2000)
6. A.W. Snow, W.R. Barger, in *Phthalocyanines: Properties and Applications*, edited by A.B.P. Lever, vol. 1 (John Wiley and Sons, New York, 1989)

https://doi.org/10.1051/epjap/2011110220 Published online by Cambridge University Press

7. L. Valli, Adv. Colloid Interface Sci. **116**, 13 (2005)
8. D. Filippini, A. Alimelli, C. DiNatale, R. Paolesse, I. Lundstrom, A. D'amico, Angew. Chem. Int. Ed. **45**, 3800 (2006)
9. J. Simon, J.-J. André, *Molecular Semiconductors* (Springer Verlag, Berlin, 1985)
10. J.-J. André, K. Holczer, P. Petit, M.-T. Riou, C. Clarisse, R. Even, M. Fourmigué, J. Simon, Chem. Phys. Lett. **115**, 463 (1985)
11. P. Turek, P. Petit, J.-J. André, J. Simon, R. Even, B. Boudgema, G. Guillaud, M. Maitrot, J. Am. Chem. Soc. **109**, 5119 (1987)
12. M. L'Her, Y. Cozien, J. Courtot-Coupez, J. Electroanal. Chem. **157**, 183 (1983)
13. M. Bouvet, E.A. Silinsh, J. Simon, Mol. Mater. **5**, 255 (1995)
14. M. Bouvet, J. Simon, Chem. Phys. Lett. **172**, 299 (1990)
15. V. Parra, M. Rei Vilar, A.M. Botelho Rego, A.M. Ferraria, S. Boufi, M.L. Rodriguez-Mendez, E. Fonavs, I. Muzikante, M. Bouvet, Langmuir **23**, 3712 (2007)
16. J. Janata, M. Josowicz, J. Solid State Electrochem. **13**, 41 (2009)
17. M. Passard, J.-P. Blanc, C. Maleysson, Thin Solid Films **271**, 8 (1995)
18. A. de Haan, M. Debliquy, A. Decroly, Sens. Actuators B Chem. **57**, 69 (1999)
19. S. Santucci, S. Picozzi, F. Di Gregorio, L. Lozzi, C. Cantalini, L. Valentini, J.M. Kenny, B. Delley, J. Chem. Phys. **119**, 10904 (2003)
20. F.I. Boher, A. Sharoni, C.N. Colesniuc, J. Park, I.K. Schuller, A.C. Kummel, W.C. Trogler, J. Am. Chem. Soc. **129**, 5640 (2007)
21. R.D. Yang, T. Gredig, C.N. Colesniuc, J. Park, I.K. Schuller, W.C. Trogler, A.C. Kummel, Appl. Phys. Lett. **90**, 263506 (2007)
22. J.A. De Saja, M.L. Rodriguez-Mendez, Adv. Colloid Interface Sci. **116**, 1 (2005)
23. V. Parra, M. Bouvet, J. Brunet, M.L. Rodriguez-Mendez, J.A. De Saja, Thin Solid Films **516**, 9012 (2008)
24. G. Guillaud, J. Simon, J.-P. Germain, Coord. Chem. Rev. **178**, 1433 (1998)
25. M. Bouvet, A. Leroy, J. Simon, F. Tournilhac, G. Guillaud, P. Lessnick, A. Maillard, S. Spirkovitch, M. Debliquy, A. de Haan, A. Decroly, Sens. Actuators B Chem. **72**, 86 (2001)
26. M. Bouvet, G. Guillaud, A. Leroy, A. Maillard, S. Spirkovitch, F.-G. Tournilhac, Sens. Actuators B Chem. **73**, 63 (2001)
27. M. Bouvet, Anal. Bioanal. Chem. **384**, 366 (2006)
28. I. Muzikante, V. Parra, R. Dobulans, E. Fonavs, J. Latvels, M. Bouvet, Sensors **7**, 2984 (2007)
29. M. Bouvet, V. Parra, C. Locatelli, H. Xiong, J. Porphyr. Phthalocyanines **13**, 84 (2009)
30. V. Parra, A.A. Arrieta, J.A. Fernandez-Escudero, H. Garcia, C. Apetrei, M.L. Rodriguez-Mendez, J.A. De Saja, Anal. Chim. Acta **563**, 229 (2006)
31. C. Apetrei, I.M. Apetrei, I. Nevares, M. Del Alamo, V. Parra, M.L. Rodriguez-Mendez, J.A. De Saja, Electrochim. Acta **52**, 2588 (2007)
32. J.-P. Germain, B. Schöllhorn, A. Pauly, C. Maleysson, J.-P. Blanc, Thin Solid Films **333**, 235 (1998)
33. J. Brunet, A. Pauly, L. Mazet, J.-P. Germain, M. Bouvet, B. Malézieux, Thin Solid Films **490**, 28 (2005)
34. B. Schöllhorn, J.-P. Germain, A. Pauly, C. Maleysson, J.-P. Blanc, Thin Solid Films **326**, 245 (1998)
35. V. Parra, J. Brunet, A. Pauly, M. Bouvet, Analyst **9**, 1776 (2009)
36. M. Bouvet, V. Parra, UPMC and CNRS, Patent FR2008/2922310 and PCT/FR2008/001325
37. Z. Bao, A.J. Lovinger, A. Dodabalapur, Appl. Phys. Lett. **69**, 3066 (1996)
38. Z. Bao, A.J. Lovinger, J. Brown, J. Am. Chem. Soc. **120**, 207 (1998)
39. D.G. De Oteyza, E. Barrena, J.O. Osso, S. Sellner, H. Dosch, J. Am. Chem. Soc. **128**, 15052 (2006)
40. D.G. De Oteyza, E. Barrena, J.O. Osso, S. Sellner, H. Dosch, J. Phys. Chem. B **110**, 16618 (2006)
41. W.J. Pietro, Adv. Mater. **6**, 239 (1994)
42. R. Murdey, N. Sato, M. Bouvet, Mol. Cryst. Liq. Cryst. **455**, 211 (2006)
43. R. Murdey, M. Bouvet, M. Sumimoto, S. Sakaki, N. Sato, Synt. Met. **159**, 1677 (2009)
44. M. Bouvet, H. Xiong, V. Parra, Sens. Actuators B Chem. **145**, 501 (2010)
45. R. Madru, G. Guillaud, M. Al Sadoun, M. Maitrot, C. Clarisse, M. Le Contellec, J.-J. André, J. Simon, Chem. Phys. Lett. **142**, 103 (1987)
46. T. Del Cano, V. Parra, M.L. Rodriguez-Mendez, R.F. Aroca, J.A. De Saja, Appl. Surf. Sci. **246**, 327 (2005)
47. M.E. Roberts, S.C.B. Mannsfeld, M.L. Tang, Z. Bao, Chem. Mater. **20**, 7332 (2008)
48. K.Y. Kondratyev, C.A. Varotsos, Environ. Sci. Pollut. R **3**, 205 (1996)
49. A. Belghachi, R.A. Collins, J. Phys. D: Appl. Phys. **23**, 223 (1990)
50. B. Timmer, W. Olthuis, A. Van den Berg, Sens. Actuators B Chem. **107**, 666 (2005)
51. J.M. Birchall, R.N. Haszeldine, J.O. Morley, J. Chem. Soc. C **19**, 2667 (1970)
52. D.D. Eley, D.J. Hazeldine, T.F. Palmer, J. Chem. Soc., Faraday Trans. 2 **69**, 1808 (1973)
53. I.S. Kirin, P.N. Moskalev, Y.A. Makashev, Russ. J. Inorg. Chem. **10**, 1065 (1965)
54. I.S. Kirin, P.N. Moskalev, Y.A. Makashev, Russ. J. Inorg. Chem. **12**, 369 (1967)
55. C. Clarisse, M.-T. Riou, Inorg. Chim. Acta **130**, 139 (1987)
56. S. Yim, T.S. Jones, Phys. Rev. B **73**, 161305 (2006)
57. D.G. De Oteyza, T.N. Krauss, E. Barrena, S. Sellner, H. Dosch, Appl. Phys. Lett. **90**, 243104 (2007)
58. S.M. Tadayyon, H.M. Grandin, K. Griffiths, P.R. Norton, H. Aziz, Z.D. Popovic, Org. Electron. **5**, 157 (2004)
59. T.C. Van Cott, Z. Gasyna, P.N. Shatz, M.E. Boyle, J. Phys. Chem. **99**, 4820 (1995)
60. E. Orti, J.-L. Brédas, C. Clarisse, J. Chem. Phys. **92**, 1228 (1990)
61. E. Orti, M.C. Piqueras, R. Crespo, J.-L. Brédas, Chem. Mater. **2**, 110 (1990)

62. T. Saito, W. Sisk, T. Kobayashi, S. Suzuki, T. Iwayanagi, J. Phys. Chem. **97**, 8026 (1993)
63. T. Basova, E. Kol'tsov, A. Hassan, A. Tsargorodoskaya, A. Ray, I. Igumenov, Phys. Stat. Sol. B **242**, 822 (2005)
64. S. Hiller, D. Schlettwein, N.R. Armstrong, D. Wohlre, J. Mater. Chem. **8**, 945 (1998)
65. Z.Z. Ho, C.Y. Ju, W.M. Hetherington III, J. Appl. Phys. **62**, 716 (1987)
66. A.K. Ray, J. Exley, Z. Ghassemlooy, D. Crowther, M.T. Ahmet, J. Silver, Vacuum **61**, 19 (2001)
67. S. Yim, S. Heutz, T.S. Jones, Phys. Rev. B **67**, 165308 (2003)
68. S. Heutz, T.S. Jones, J. Appl. Phys. **92**, 3039 (2002)
69. M.L. Rodriguez-Mendez, Y. Gorbunova, J.A. De Saja, Langmuir **18**, 9560 (2002)
70. K.M. Lau, J.X. Tang, H.Y. Sun, C.S. Lee, S.T. Lee, D. Yan, Appl. Phys. Lett. **88**, 173513 (2006)
71. R. Ye, M. Baba, K. Suzuki, K. Mori, Jpn. J. Appl. Phys. **46**, 2878 (2007)
72. H. Ishii, K. Sugiyama, E. Ito, K. Seki, Adv. Mater. **11**, 605 (1999)
73. Y. Tanaka, K. Kanai, Y. Ouchi, K. Seki, Org. Electr. **10**, 990 (2009)
74. T. Manaka, M. Iwamoto, Thin Solid Films **438**–**439**, 157 (2003)
75. G. Guillaud, M. Al Sadoun, M. Maitrot, J. Simon, M. Bouvet, Chem. Phys. Lett. **167**, 503 (1990)
76. J. Wang, H. Wang, J. Zhang, X. Jan, D. Yan, J. Appl. Phys. **97**, 026106 (2005)
77. J.-P. Germain, A. Pauly, C. Maleysson, J.-P. Blanc, B. Schollhörn, Thin Solid Films **333**, 235 (1998)
78. B.A. Jones, A. Facchetti, M.R. Wasielewski, T.J. Marks, J. Am. Chem. Soc. **129**, 15259 (2007)
79. A. Facchetti, Mater. Today **10**, 28 (2007)
80. Y. Chen, M. Bouvet, T. Sizun, G. Barochi, J. Rossignol, E. Lesniewska, Sens. Actuators B Chem. **155**, 165 (2011)

https://doi.org/10.1051/epjap/2011110220 Published online by Cambridge University Press